J Mol Model (2007) 13:651–663
DOI 10.1007/s00894-007-0215-6

ORIGINAL PAPER

The field theoretical study of chemical interaction in terms of the Rigged QED: new reactivity indices

Paweł Szarek · Akitomo Tachibana

Received: 15 November 2006 / Accepted: 3 May 2007 / Published online: 30 May 2007

Abstract How the mode of bonding affects stability and reactivity of molecule on the frame of nonrelativistic limit of the rigged quantum electrodynamics using new indices for description of bond properties related to bond orders have been characterized here. These indices are in close relation with tensorial interpretation of bond that among others allows discriminating covalent bonds using spindle structure concept. The real three-dimensional space representation of new interaction energy density utilized in this study contribute to better understanding of interaction phenomena between atoms and molecules. The differences in reactivity and stabilities of molecules have their root in the redistribution of interaction energy density.

Keywords Bond line · Bond order · Energy density · Interaction energy · Lagrange point · Reactivity · Reactivity indices · Regional chemical potential

Introduction

The recently developed novel field theory of regional energy density decomposition in real space [1–5] (an infinitely small regional energy decomposition scheme) [6–9] allows one to recognize how the electronic energy density is associated with the electron density and visualization of the chemical interaction in real space is now possible. Using the electronic energy density, one can pick up any point in a chemical reaction system and find how the electronic energy E is assigned to that point. The integration of the electronic energy density in a small region gives the regional electronic energy contribution to the global electronic energy E. If the integration spans the whole space, then the integral gives the total E of system. The new energy density partitioning scheme that utilizes rigged quantum electrodynamics (QED) has been developed recently [1–5]. One obtains the energy densities as follows:

$$n_E(\vec{r}) = n_T(\vec{r}) + n_V(\vec{r}) + n_W(\vec{r}) \tag{1.1a}$$

$$n_E(\vec{r}) = \left\langle \hat{H}(\vec{r}) \right\rangle, n_T(\vec{r}) = \left\langle \hat{T}(\vec{r}) \right\rangle,$$
$$n_V(\vec{r}) = \left\langle \hat{V}(\vec{r}) \right\rangle, n_W(\vec{r}) = \left\langle \hat{W}(\vec{r}) \right\rangle \tag{1.1b}$$

the kinetic energy density $n_T(\vec{r})$, the external potential energy density $n_V(\vec{r})$, and the interelectron potential energy density $n_W(\vec{r})$. The components are derived from the same density matrix and related to each other following the sum rule that leads to the total energy density $n_E(\vec{r})$.

The kinetic energy density obtained in this scheme provides a new outlook at the chemical bond by partitioning of space into mutually disjoint regions by using a concept of the electronic drop (R_D) and atmosphere (R_A) regions separated by the interface S [10]. The infinitely large positive electric potential of the bare nucleus influences the electron (in terms of classical and quantum mechanics as well) that has constant energy and can acquire infinitely large positive kinetic energy $n_T(\vec{r})$ at positions very near to nucleus (because the intramolecular electric field $E_{intra}(\vec{r})$ produced by the other electrons can not exceed that of the bare nucleus) [6–9]. Nevertheless the nucleus is surrounded by the surface of zero kinetic energy

P. Szarek · A. Tachibana (✉)
Department of Micro Engineering, Kyoto University,
Kyoto 606-8501, Japan
e-mail: akitomo@scl.kyoto-u.ac.jp

density $\left(n_T(\vec{r})=0\right)$, within which the kinetic energy density is positive $\left(n_T(\vec{r})>0\right)$, where the electron density is simply accumulated and classically allowed motion of electron is guaranteed. This region is called the electronic drop and denoted by R_D, while the complementary region is the region of the electronic atmosphere denoted by R_A, being separated by the electronic interface S:

$$n_T(\vec{r}) = -\frac{\hbar^2}{4m}\sum_i^{occ}\nu_i\left[\psi_i^*(\vec{r})\Delta\psi_i(\vec{r}) + \Delta\psi_i^*(\vec{r})\psi_i(\vec{r})\right] \tag{1.2a}$$

$$\begin{array}{l} R_D : n_T(\vec{r}) > 0 \\ R_A : n_T(\vec{r}) < 0 \\ S : n_T(\vec{r}) = 0 \end{array} \tag{1.2b}$$

In the R_A the electron density is dried up and the motion of electrons is classically forbidden. The boundary S in between R_D and R_A gives a clear image of the intrinsic shape of the reactant atoms and molecules along the course of the chemical reaction coordinate. The kinetic energy density is a molecular property as a functional of electron density [1, 11–13]. While expectation values in the whole space of both conventional (regular DFT) and the Rigged QED kinetic energy density operators are the same, the density itself is different from each other [2]. The interface surface S, that appears for the rigged QED $n_T(\vec{r})$, is very important in chemical reaction systems as it allows specifying the turning point for electron [14].

The dynamical treatment, in the form of incorporation of the kinetic energy density of atomic nuclei (treated as external static source of force for electrons-Schrödinger field [15]), plays an important role in the rigged QED in the chemical reaction systems since the local stress tensor density $\overleftrightarrow{\tau}^S(\vec{r})$, represented as force acting on a pair of electronic drop regions of reactants [10, 16], have been applied to study the chemical reactivity [17]:

$$\overleftrightarrow{\tau}^S(\vec{r}) = \left\langle \widehat{\overleftrightarrow{\tau}}^S(\vec{r}) \right\rangle \tag{1.3a}$$

$$\tau^{Skl}(\vec{r}) = \frac{\hbar^2}{4m}\sum_i^{occ}\nu_i \left[\psi_i^*(\vec{r})\frac{\partial^2\psi_i(\vec{r})}{\partial x^k\partial x^l} - \frac{\partial\psi_i^*(\vec{r})}{\partial x^k}\frac{\partial\psi_i^*(\vec{r})}{\partial x^l} + \frac{\partial^2\psi_i^*(\vec{r})}{\partial x^k\partial x^l}\psi_i(\vec{r}) - \frac{\partial\psi_i^*(\vec{r})}{\partial x^l}\frac{\partial\psi_i^*(\vec{r})}{\partial x^k}\right] \tag{1.3b}$$

The eigenvalue is the principal stress and the eigenvector is the principal axis:

$$\left\langle \widehat{\overleftrightarrow{\tau}}^S(\vec{r}) \right\rangle = \begin{bmatrix} \tau_{xx}^S(\vec{r}) & \tau_{xy}^S(\vec{r}) & \tau_{xz}^S(\vec{r}) \\ \tau_{yx}^S(\vec{r}) & \tau_{yy}^S(\vec{r}) & \tau_{yz}^S(\vec{r}) \\ \tau_{zx}^S(\vec{r}) & \tau_{zy}^S(\vec{r}) & \tau_{zz}^S(\vec{r}) \end{bmatrix} \xrightarrow{diag} \begin{bmatrix} \tau^{S11}(\vec{r}) & 0 & 0 \\ 0 & \tau^{S22}(\vec{r}) & 0 \\ 0 & 0 & \tau^{S33}(\vec{r}) \end{bmatrix} \tag{1.4a}$$

$$\tau^{S11}(\vec{r}) \le \tau^{S22}(\vec{r}) \le \tau^{S33}(\vec{r}) \tag{1.4b}$$

This new kind of force which acts on electrons is discriminated with the force on the nuclei. The covalent bond formation is characterized by a concept of the spindle structure, which is a geometrical object of a region where principal electronic tensile stress is positive along the line of principal axis of the electronic stress, that connects a pair of the R_D's of atoms or molecules (with predominant compressive stress inside) [16].

The stress is the surface force characterized by the dimension of force per area. The eigenvector of the stress tensor density dictates the local tensorial chemical force.

The eigenvalue of the stress tensor density gives a measure of the kinetic energy. If the local principal stress is positive, it is called the tensile stress, while if it is negative-compressive [16]. The compressive stress gives a positive contribution to the kinetic energy density, while the tensile stress provides a negative contribution because of negative eigenvalues (−1, −1, −1) of metric tensor g_{ij} [14]. Combination of the stress tensor and the spindle structure reveals new concept of tensorial chemical interaction energy density that includes the electronic spin angular momentum in the underling physics. The atomic electron density exhibits positive kinetic energy density, which leads to the formation of the electronic drop region R_D [10] and to the compressive stress [16]. This tendency should of course be intact in between ionic species interactions. The situation would change dramatically for covalent bond formation, where a pair of electrons should be bound tightly and thereby creating tensile stress. Many systems show such generic feature, which is called spindle structure of covalent bond [15].

On the basis of the concept of the force density and the stress density (established in the quantum mechanics and QED), the force density operator $\overrightarrow{F}^S(r)$, aside form the Lorentz force density operator $\overrightarrow{L}^S(\vec{r})$, is composed of the tension density operator $\overrightarrow{\tau}^S(\vec{r})$ given as the divergence of

the stress tensor density operator $\widehat{\overrightarrow{\tau}}^{S}(\overrightarrow{r})$:

$$\hat{\tau}^{Sk}(\overrightarrow{r}) = \partial_l \hat{\tau}^{Skl}(\overrightarrow{r}) \tag{1.5}$$

$$\widehat{\overrightarrow{F}}^{S}(r) = \widehat{\overrightarrow{\tau}}^{S}(\overrightarrow{r}) + \widehat{\overrightarrow{L}}^{S}(\overrightarrow{r}). \tag{1.6}$$

Tension density operator represents purely quantum mechanical effects, for example, of electrons diffusing from an atomic nucleus. The Lorentz force density operator is of the usual classical form plus quantum mechanical exchange effects, for example, of electrons pulled back by the atomic nucleus. For the stationary state of charged particles the local force can vanish, when the equation of motions is equivalent to the local equilibrium condition and where the tension density (the tension of the field) exactly cancels the Lorentz force density (the Lorentz force exerted on the particle) at every point of space [10, 14, 16, 18]:

$$\left\langle \widehat{\overrightarrow{\tau}}^{S}(\overrightarrow{r}) \right\rangle + \left\langle \widehat{\overrightarrow{L}}^{S}(\overrightarrow{r}) \right\rangle = 0. \tag{1.7}$$

The tension is integrable, and leads to the stress tensor, which itself has the dimension of the energy density:

$$[\text{stress}] = \frac{\text{force}}{\text{area}} = \frac{\text{energy}}{\text{volume}} = [\text{energy density}]. \tag{1.8}$$

Regional energy density

Bond line and lagrange point

In the stress tensor analysis, one can visualize the propagation of local force in real space by tracing the congruence of the principal axes, leading to the bond line as the envelope, as shown in Fig. 1a. The spindle structure accommodates a bundle of bond lines carrying tensile stress region in between a pair of compressive ones on the edges with a shape of bond if they connect a pair of R_D's.

In Bader's analysis topologically defined bond paths, bond critical points and electron cloud enclosed regions serve as regions of space carrying the information about bonding interaction and atomic regions [23]. The rigged QED analysis at stationary point provides the chemical interaction characteristic with the Lagrange point $\overrightarrow{r}_{Lagrange}$ at which the tension (and also the Lorentz force) vanishes for electron to take a rest in course of the chemical bond, as shown in Fig. 1b. We suggest that $\overrightarrow{r}_{Lagrange}$ carries a heavy load of interaction information, however it may not be complete. The $\overrightarrow{r}_{Lagrange}$ are common for all molecules and easy to identify. In contrast to Bader's AIM analysis [23] the rigged QED characteristic point is determined by dynamical forces acting on electrons thus has mechanical origin instead of being a topological parameter.

Concluding, one obtains: i) a realization of boundaries of atoms or other electronic structural fragments as the R_D - drop regions of kinetic energy density separated with R_A , ii) a dynamical bond line dictating the local tensorial chemical force, and iii) a dynamical point $\overrightarrow{r}_{Lagrange}$ characterizing an interaction, where repulsive electronic tension cancels in space (in stationary state) [15]. The kinetic energy density can draw a shell structure of atoms. The tangential point of two atoms or molecules is called Lagrange point $\overrightarrow{r}_{Lagrange}$ and it is situated on the bond line that connects two R_D centers.

Non-relativistic limit of energy density

Tensorial analysis of bonding interactions has already been proved to be useful in determination of covalence and molecular shape [10]. Because the stress tensor has a dimension of the energy density, a completely new realization of the tensorial chemical interaction energy density was obtained. The trace of the stress tensor density becomes [15] equivalent to two times the kinetic energy density in the non-relativistic limit. The integral of the trace of the stress tensor density gives a local picture of two times the kinetic energy density [15].

$$E_{Rigged\ QED} = \int d^3\overrightarrow{r} \left\langle \hat{H}_{Rigged\ QED}(\overrightarrow{r}) \right\rangle$$
$$= \int d^3\overrightarrow{r} \left\langle m_e c^2 \widehat{\overline{\psi}}(\overrightarrow{r}) \hat{\psi}(\overrightarrow{r}) - \sum_{\alpha} \hat{T}_{\alpha}(\overrightarrow{r}) \right\rangle \tag{2.1}$$

$$E^{\ non-relativistic}_{\ Rigged\ QED}$$
$$= \int d^3\overrightarrow{r} \left\langle \hat{H}^{\ non-relativistic}_{\ Rigged\ QED}(\overrightarrow{r}) \right\rangle$$
$$= -\frac{1}{2} \int d^3\overrightarrow{r} \left\langle \sum \hat{\tau}^{Sk}_{\alpha k}(\overrightarrow{r}) \right\rangle. \tag{2.2}$$

The quantity calculated in this way corresponds to the total electronic energy E (when integration spans the whole space). Its local redistribution in space (ε-total energy density) can be drawn by using regional integration for infinitively small region of space [1–5]:

$$E = \int d^3\overrightarrow{r} \varepsilon^{S}_{\tau}(\overrightarrow{r}), \quad \varepsilon^{S}_{\tau}(\overrightarrow{r}) = \frac{1}{2} \tau^{Skk}(\overrightarrow{r}). \tag{2.3}$$

Lagrange point vs. regional energy density

The total energy density in local picture reaches peak along the principal axis (bond line) in the $\overrightarrow{r}_{Lagrange}$ and for perpendicular axis leading through this point goes through

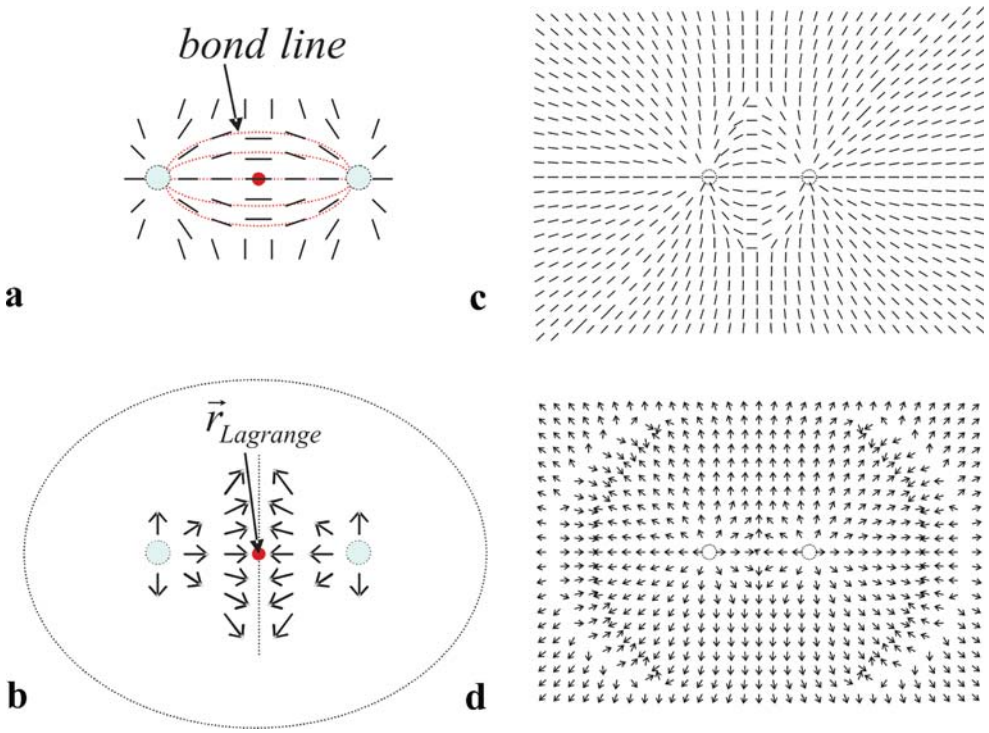

Fig. 1 The bond lines and Lagrange point $\vec{r}_{Lagrange}$; **a**) the eigenvectors of principal stress constitute the bond lines, **b**) the cancellation of tension defines Lagrange point (situated on a bond line), **c**) the eigenvectors of principal stress tensor arranged in bond lines in H_2 molecule, and **d**) tension cancellation in between atoms

the minima. It is not a necessary condition that electron density would go through the extremum at $\vec{r}_{Lagrange}$ too, especially in many atomic or heteroatomic systems. The b_ε value of ratios of energy densities at this point, calculated from the equation below, where $\varepsilon^S_{\tau AB}(\vec{r}_{Lagrange})$ is the regional energy density at $\vec{r}_{Lagrange}$ for bond between A and B, and $\varepsilon^S_{\tau HH}(\vec{r}_{Lagrange})$ is regional energy density at $\vec{r}_{Lagrange}$ for σ bond in a hydrogen molecule, is linked to bond order (defined in diatomic molecule as b=1/2(n-n*)) or more precisely to normalized interatomic strain (which may be compared to vacuum pressure) that glues atoms together, stabilizing given bonding interaction with respect to the properties of model pure single σ bond of a hydrogen molecule.

$$b_\varepsilon = \frac{\varepsilon^S_{\tau AB}(\vec{r}_{Lagrange})}{\varepsilon^S_{\tau HH}(\vec{r}_{Lagrange})} \tag{2.4}$$

Table 1 shows results for Lagrange points of carbon-carbon bond of C_2H_x molecules and model single bond of H_2 molecule, all calculated at MP2/6-311++G** level of theory using Gaussian03 [24] and MRDFT program [25]. The largest eigenvalue of stress is positive for all cases except etyn, for which it is slightly negative - this is due to the effect of large stabilization in the directions perpendicular to the bond line that cause the covering up of tensile stress in the principal axis. The positive stress is delocalized from the $\vec{r}_{Lagrange}$ into the ring shaped region around bond axis. The two minor eigenvalues of stress tensor are negative and represent the compressive stress acting on bonding electrons in directions perpendicular to C-C line. The negativity of these eigenvalues is connected with atomic like stabilization, while positive stress is associated with electronic destabilization (or stabilization in sense of tight covalent bonding of valence electrons). The electron density at $\vec{r}_{Lagrange}$ correlates with increasing b_ε. The values of b_ε are in good agreement with bond orders in these molecules. The results for other C-C bonds in hydrocarbons i.e.: s-trans-1,3-buten ($b_\varepsilon = 1.274$ and 1.897 for single and double respectively) or $\vec{r}_{Lagrange}$ between C atoms in benzene molecule ($b_\varepsilon = 1.557$) also assume reasonable values that correlate with bond orders. It should be noted that negativity of the largest eigenvalue of stress at $\vec{r}_{Lagrange}$ does not necessary negate the covalence and spindle structure existence. The largest eigenvalue of stress tensor is negative for non-covalent interactions (metallic bonds, van der Waals complexes) or sometimes for very strong covalent bonds where short interatomic distance causes that positive principal stress is dominated by compressive stresses of atomic cores. The value for etyn molecule turns out to be negative as the total result of superimposed effects. The negativity of principal stress in this case might mean fluidity of electron density and potential to conduct (see next paragraph for more information). It is possible however to find the spindle structure when electronic "noise" in shape of all occupied orbitals except HOMO will be omitted [14].

Homonuclear diatomic molecules

The homonuclear diatomic molecules in ground states of main group elements, from first to fourth period, have been

Table 1 The Lagrange point characteristics of C-C bonds-eigenvalues of stress tensor, electron density and regional total energy density (in atomic units)

Molecule	The eigenvalues of stress tensor			Electron density	Total energy density	b_ε	b_μ
H_2	1.7190E-01	−2.2420E-01	−2.2420E-01	2.6430E-01	−1.3825E-01	1.00	1.00
C_2H_6	6.0200E-02	−1.6410E-01	−1.6410E-01	2.5060E-01	−1.3400E-01	0.97	1.02
C_2H_4	4.0530E-02	−2.6950E-01	−3.0820E-01	3.4580E-01	−2.6859E-01	1.94	1.48
C_2H_2	−9.8110E-03	−4.1060E-01	−4.1060E-01	3.9690E-01	−4.1551E-01	3.01	2.00

The b_ε ratio correlates with the bond orders of C-C bonds while modified index b_μ does not work for multiple bonds.

analyzed here with respect to the Lagrange point. The results are shown in Table 2. The calculations have been performed at HF/6-311++G** level of theory using Gaussian03 [24] and MRDFT program [25]. The regional total energy density as well as b_ε reflect periodicity of atomic properties and correlate with bond length and electron density at Lagrange points. Among the elements of the first two groups one can notice that from Na_2 to Ca_2 the degeneracy of the largest eigenvalue occurs in contrast to the degeneracy of two minor eigenvalues of stress in other cases. There also appears another clear tendency, that among all metals and metalloids bonds the largest eigenvalue of stress in Lagrange point becomes negative. This indicates a kind of fluidity of bonding/valance electron density between species. There might be a connection between such a feature and band properties of metals and semiconductors however not studied yet.

The b_ε index does not give commonly used bond orders any more. While it still evaluates the bond strength and order, the magnitude for some bonds is either largely overestimated or underestimated comparing to results by Mayer's [26–29] or molecular orbital theory [30–33]. One can obtain more adequate results by taking dependency of electron redistribution into consideration since the electronic energy is associated with electron density [18–22]. The modified index takes also the interaction of electronic clouds of bonding species into account. In chemical reaction systems, the redistribution of electrons directly redefines the electronic energy as a unique functional of the electron density [10]. New parameter is calculated from equation below, where $n_{AB}(\vec{r}_{Lagrange})$ indicates electron density at $\vec{r}_{Lagrange}$ for given bond.

$$b_\mu = \frac{b_\varepsilon}{\left(n_{AB}(\vec{r}_{Lagrange})/n_{HH}(\vec{r}_{Lagranre})\right)} = \frac{\varepsilon^S_{\tau AB}(\vec{r}_{Lagranre})}{n_{AB}(\vec{r}_{Lagranre})} \cdot \left(\frac{\varepsilon^S_{\tau HH}(\vec{r}_{Lagranre})}{n_{HH}(\vec{r}_{Lagranre})}\right)^{-1}. \quad (2.5)$$

The ε/n ratio reflects energy that is attributed to one electron at given point in space. For particular interaction between two R_D's the $\vec{r}_{Lagrange}$ describes exclusively only that particular phenomenon (especially if one investigates bonding in composed, many-atomic system). One can easily compare normalized energy density (first, bond order related parameter) or such energy per one electron at atomic (or molecular) interfaces expressed by any interacting subsystem.

Linear response of regional chemical potential density

The regional energy decomposition scheme has been extended to infinitely small regional energy decomposition scheme thus leading to local electronic energy density $n_E(\vec{r})$ in real space as a unique functional of electron density $n(\vec{r})$ [1, 2, 18–22, 34]. In this sense $\varepsilon^S_{\tau AB}(\vec{r})$ constitutes a very small, partial contribution (∂E) to total electronic energy, likewise $n_{AB}(\vec{r})$ makes a small portion (∂N) of total electron number N, for a given region of space for bond between A and B:

$$E_{AB} = \int d^3\vec{r}\,\varepsilon^S_{\tau AB}(\vec{r}), N_{AB} = \int d^3\vec{r}\, n_{AB}(\vec{r}). \quad (2.6)$$

However the ratio of energy density per electron density has a much deeper meaning and broader importance for chemical description of the system at a single point of space. The $\varepsilon^S_{\tau AB}(\vec{r})/n_{AB}(\vec{r})$ in Eq. (2.5) may be regarded as derivative versus number of electrons that exhibits the property of regional chemical potential (μ_R) [1] at least under linear response approximation:

$$\mu_R = \left(\frac{\partial E_R}{\partial N_R}\right) \Leftrightarrow \frac{\varepsilon^S_{\tau AB}(\vec{r})}{n_{AB}(\vec{r})}. \quad (2.7)$$

The original Onsager's local equilibrium hypothesis that does not include quantum mechanical effects across region interfaces [35, 36] has been modified, and the quantum mechanical nature of the electron was taken into account by use of density functional theory [1]. Introduction of quantum mechanical coherency of electrons that can tunnel from region R to the neighboring regions allow replacing all Hamiltonians (originally for each region) by one density functional theory Hamiltonian that covers the system as a whole. In the irreversible thermodynamic of Onsager, there is a gradient of chemical potentials and there is an

Table 2 Periodicity of the stress tensor and energy density related parameters at Lagrange point

	H_2							He_2
3rd eigenvalue of stress tensor	0.1738							−0.000019
2nd eigenvalue of stress tensor	−0.2269							−0.000028
1st eigenvalue of stress tensor	−0.2269							−0.000028
Electron density	0.2660							0.000123
Regional total energy density	−0.1400							−0.000032
b_ε	1							0.00027
b_μ	1							0.579
Electron density difference	0.1080							−2.60E-07
Interaction energy density	−0.0664							−4.36E-07
$b_{\Delta\varepsilon}$	1							6.57E-06
Interatomic distance [Å]	0.74							3.68
	Li_2	Be_2	B_2	C_2	N_2	O_2	F_2	Ne_2
3rd eigenvalue of stress tensor	−0.0008	−0.0149	−0.0045	0.0057	0.0908	0.3861	0.308	−0.000130
2nd eigenvalue of stress tensor	−0.001	−0.0159	−0.0571	−0.2011	−1.09	−0.9308	−0.4539	−0.000407
1st eigenvalue of stress tensor	−0.001	−0.0159	−0.0571	−0.2011	−1.09	−0.9308	−0.4539	−0.000407
Electron density	0.0129	0.0725	0.111	0.2008	0.7321	0.629	0.3563	0.001051
Regional total energy density	−0.0014	−0.0234	−0.0594	−0.1983	−1.0446	−0.7378	−0.2999	−0.000473
b_ε	0.010	0.167	0.424	1.416	7.462	5.270	2.142	0.00338
b_μ	0.214	0.613	1.015	1.876	2.711	2.228	1.599	0.854
Electron density difference	0.0070	0.0326	−0.0446	−0.0814	0.1855	−0.1010	−0.0787	−1.14E-05
Interaction energy density	−0.0018	−0.0271	–	–	−0.7044	–	–	−2.15E-05
$b_{\Delta\varepsilon}$	0.027	0.408	–	–	10.615	–	–	0.000325
Interatomic distance [Å]	2.78	1.81	1.64	1.36	1.07	1.16	1.33	3.27
	Na_2	Mg_2	Al_2	Si_2	P_2	S_2	Cl_2	Ar_2
3rd eigenvalue of stress tensor	−0.0005	−0.0033	−0.0111	−0.0138	−0.0449	0.007	0.043	−0.000016
2nd eigenvalue of stress tensor	−0.0005	−0.0033	−0.0136	−0.0335	−0.1076	−0.1229	−0.0924	−0.000034
1st eigenvalue of stress tensor	−0.0007	−0.0064	−0.0136	−0.0335	−0.1076	−0.1229	−0.0924	−0.000034
Electron density	0.0084	0.0273	0.0459	0.0664	0.194	0.2013	0.157	0.000202
Regional total energy density	−0.0009	−0.0065	−0.0192	−0.0405	−0.1301	−0.1194	−0.0709	−0.000042
b_ε	0.006	0.046	0.137	0.289	0.929	0.853	0.506	0.00030
b_μ	0.196	0.452	0.792	1.156	1.274	1.127	0.857	0.392
Electron density difference	0.0038	0.0076	−0.0168	−0.0285	0.0565	−0.0137	−0.0138	0
Interaction energy density	−0.0008	−0.0060	–	–	−0.1140	–	–	0.0022
$b_{\Delta\varepsilon}$	0.013	0.090	–	–	1.717	–	–	–
Interatomic distance [Å]	3.20	2.53	2.25	2.05	1.85	1.88	2.00	5.03
	K_2	Ca_2	Ga_2	Ge_2	As_2	Se_2	Br_2	Kr_2
3rd eigenvalue of stress tensor	−0.0002	−0.0015	−0.0071	−0.0139	−0.0334	−0.0083	0.0122	−0.000010
2nd eigenvalue of stress tensor	−0.0002	−0.0015	−0.0128	−0.0334	−0.0681	−0.0626	−0.0508	−0.000021
1st eigenvalue of stress tensor	−0.0003	−0.0019	−0.0154	−0.0334	−0.0681	−0.0626	−0.0508	−0.000021
Electron density	0.0044	0.0144	0.0518	0.0596	0.141	0.1339	0.1128	0.000154
Regional total energy density	−0.0004	−0.0033	−0.0096	−0.0202	−0.0650	−0.0597	−0.0354	−0.000021
b_ε	0.002	0.017	0.126	0.288	0.606	0.477	0.319	0.00019
b_μ	0.145	0.322	0.648	1.287	1.143	0.947	0.752	0.324
Electron density difference	0.0019	0.0043	−0.0038	−0.0329	0.0263	−0.0216	−0.0081	−6.40E-07
Interaction energy density	−0.0003	−0.0020	–	–	−0.0442	–	–	−4.90E-07
$b_{\Delta\varepsilon}$	0.004	0.030	–	–	0.666	–	–	7.38E-06
Interatomic distance [Å]	4.20	3.35	2.54	2.18	2.06	2.15	2.29	5.58

inequality of regional chemical potentials between complementary regions. The introduced quantum mechanical interference effect, working through the interfaces that divide the regions, survives even in the limit of global chemical equilibrium [1]. Arising chemical potential inequality principle predicts inequality in between either: i) the Gibbs chemical potential μ_G for electronic subsystem as a whole and the regional chemical potentials μ_R, or ii) the regional chemical potentials μ_R themselves [1].

$$\mu_G = \mu_R + \sum_{R'(\neq R)} \alpha_{R'R} \tag{2.8}$$

$$\mu_R = \left(\frac{\partial E_R}{\partial N_R}\right)_{S,v,N_{R'(\neq R)}} \tag{2.9}$$

$$\alpha_{R'R} = \left(\frac{\partial E_{R'}}{\partial N_R}\right)_{S,v,N_{R'(\neq R)}} \tag{2.10}$$

The μ_R refers to regional contribution to the μ_G. The sum of $\alpha_{R'R}$ over the complementary regions R' to R expresses intrinsic Volta electric potential ϕ_R. For a pair of regions R' and R Volta contact potential difference is identified with the difference in the regional work function proved by Herring and Nichols [37].

$$\phi_R - \phi_{R'} = \Phi_{R'} - \Phi_R \tag{2.11}$$

The Φ_R denotes the intrinsic Herring-Nichols work function. In between a pair of regions in contact with each other, the Gibbs chemical potential is constant as a consequence of the chemical equilibrium. This leads to Herring-Nichols work function Φ_R defined as regional chemical potential.

$$\mu_G = -e\Phi_R - e\phi_R = -e\Phi_{R'} - e\phi_{R'} \tag{2.12}$$

$$-e\phi_R = \sum_{R'(\neq R)} \alpha_{R'R} \tag{2.13}$$

$$-e\Phi_R = \mu_R \tag{2.14}$$

The thermodynamic extension of electronic energy density $n_E(\vec{r})$ gives observables in electrochemistry in the shape of ϕ_R and Φ_R. Likewise in crystals where these quantities are dependent on surface morphologies or crystallographic orientations but have a constant value of μ_G, the same regional chemical potential inequality in space for atoms and molecules is a valuable source of chemical interaction information.

According to Ilya Prigogine an open system at stationary state organizes itself in a way to minimize total entropy production. The thermodynamic forces represented by gradients of intensive variables drive fluxes of the associated extensive quantities [1]. The μ_G turns out to be electrochemical potential composed of ordinary chemical potential arising from short range interactions and the macroscopic scalar electric potential field ϕ representing long range electromagnetic interactions [38]. The two parts of the electrochemical potential play a different role in thermodynamics [38].

Figure 2 compares b_ε and b_μ indices with the molecular orbital theory bond orders [30–33]. The modified index b_μ describes the actual bond orders more accurately. However this new index, due to underestimation, is now not applicable to the carbon-carbon bonds in hydrocarbons (Table 1). This is due to the effect caused by bonding to more then one atomic center, when electron density may redistribute over the whole, much larger molecular orbital that spans all the nuclei. In diatomic molecules, where available orbital space is limited comparing to polyatomic molecules, electron density accumulated around one particular bond, although may not exceed that for similar bond in polyatomic system, has more favorable energy (due to lower number of available/occupied MOs; i.e., carbon-carbon bond in C_2 and hydrocarbons) thus this causes change in local chemical potential at $\vec{r}_{Lagrange}$ and related b_μ index.

Method and basis set dependency

The calculations of energy density data are based on the eigenvectors obtained from any *ab initio* method implemented in commercially available programs for quantum mechanical calculations and the same basis sets are used. The dependency on method and basis set have been checked by HF, MP2, and B3LYP calculations with STO-3G, 6-31G, 6-311G basis sets (with polarization and diffusion functions added or removed) using Gaussian 03 [24] and MRDFT program [25]. The very small method and small basis set dependency have been observed. The results for Li_2 case have been summarized in Table 3. In the case of constant interatomic distance all methods give very similar results and the regional total energy density at HF and B3LYP levels correlate very well (1.000 and 0.995 respectively) with MP2 results for the H_2 molecule.

Interaction energy density

The combination of supermolecular approach and non-relativistic limit of energy density leads to the formulation of new molecular interaction energy density of the chemical species (corrected for the basis set superposition error (BSSE) by using the dimmer centered basis set for monomers [39]). This new energy density is divided into the regions where attractive or repulsive interaction terms are dominating, that in case of bonding interaction might be regarded as stabilization or destabilization in bonding regions respectively, as the effect of electron density rearrangement upon bond formation.

$$\Delta E_{AB} = E_{AB} - (E_A + E_B) \tag{2.15}$$

The corresponding value of local molecular interaction energy density is defined as follows:

$$\Delta\varepsilon^S_{\tau AB}(\vec{r}) = \varepsilon^S_{\tau AB}(\vec{r}) - \left(\varepsilon^S_{\tau A}(\vec{r}) + \varepsilon^S_{\tau B}(\vec{r})\right) \tag{2.16}$$

This approach has been applied recently to study hydrogen bond interactions for visualization of intermolec-

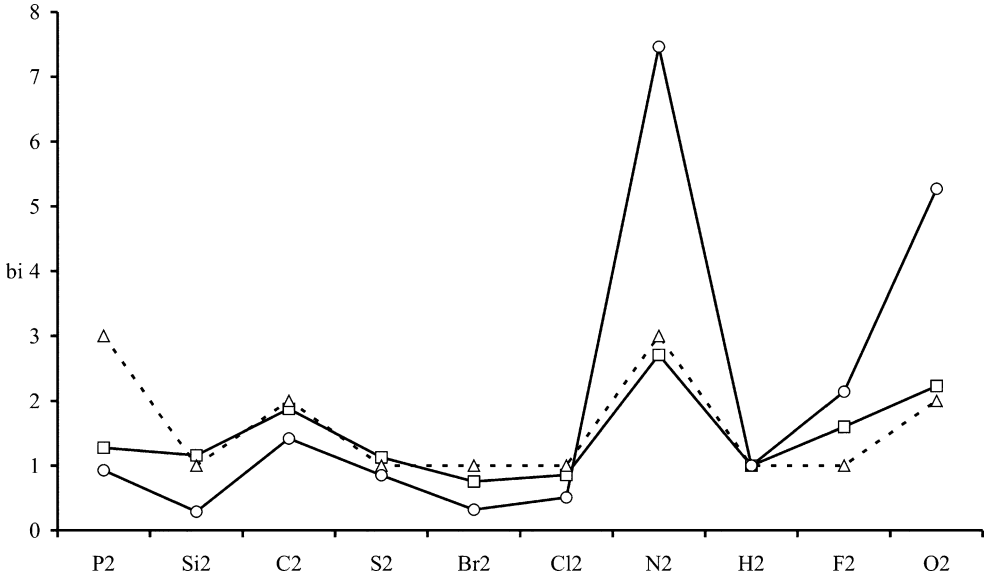

Fig. 2 Comparison of MO theory bond orders (b=(n-n*)/2)- doted line with b_ε (circles) and b_μ (squares). The molecules are ordered according to the increasing largest eigenvalue of stress tensor at Lagrange point

ular effects between donor and acceptor pair [to be published].

Similarly to the regional total energy density and b_ε index it is possible to define ratio of molecular interaction energy densities:

$$b_{\Delta\varepsilon} = \frac{\Delta\varepsilon^S_{\tau AB}\left(\overrightarrow{r}_{Lagrange}\right)}{\Delta\varepsilon^S_{\tau HH}\left(\overrightarrow{r}_{Lagrange}\right)} \tag{2.17}$$

The $b_{\Delta\varepsilon}$ represents the relative stability of given A-B bond comparing to single σ bond of hydrogen molecule. In other words the character (passive-quite stable, or aggressive-quite unstable) of interaction and tendency to undergo transformation from given stationary state is characterized. The change of this index with respect to the standard bond energies is presented in Fig. 3. One can notice from data in Table 2 that the lowest value of $b_{\Delta\varepsilon}$ is attached to bond in Kr_2 molecule which is very weakly bonded. In contrast the most inert among molecules in Table 2 the N_2 has the highest value. This index describes how much the given bond is stabilized comparing to single H-H bond, in other words the effect of localization of bonding electrons in space in between nuclei is evaluated. For example Li_2 and Be_2 molecules have less stable but energetically favorable interaction at $\overrightarrow{r}_{Lagrange}$. The interaction in N_2 is estimated to be much stronger then in H_2 and electronic type interaction is exclusively localized in between nitrogen atoms. The negativity of this index would mean destabilizing effects present at $\overrightarrow{r}_{Lagrange}$ (thus high reactivity) or indicate delocalization of bonding (attractive, electronic) interactions to the regions outside interatomic axis. In this case three-dimensional view is needed to fully illustrate bonding interaction character.

Table 3 The method and basis set dependency of b_ε and b_μ for Li_2

	STO-3G	6-31G	6-31++G	6-31G**	6-31++G**	6-311G	6-311++G	6-311G**	6-311++G**
R [Å]									
B3LYP	2.6888	2.7325	2.7334	2.7230	2.7254	2.7055	2.7056	2.7048	2.7050
HF	2.6964	2.8155	2.8218	2.8069	2.8145	2.7846	2.7847	2.7844	2.7846
MP2	2.6994	2.8109	2.8154	2.7821	2.7872	2.7698	2.7687	2.7485	2.7479
b_ε									
B3LYP	0.017	0.010	0.010	0.009	0.009	0.013	0.013	0.013	0.013
HF	0.016	0.008	0.008	0.008	0.007	0.011	0.011	0.010	0.010
MP2	0.017	0.008	0.008	0.008	0.008	0.011	0.011	0.011	0.011
b_μ									
B3LYP	0.252	0.168	0.170	0.170	0.167	0.220	0.220	0.214	0.214
HF	0.278	0.193	0.195	0.191	0.190	0.248	0.248	0.244	0.244
MP2	0.268	0.173	0.176	0.173	0.172	0.227	0.228	0.223	0.224

Data in atomic units unless marked otherwise

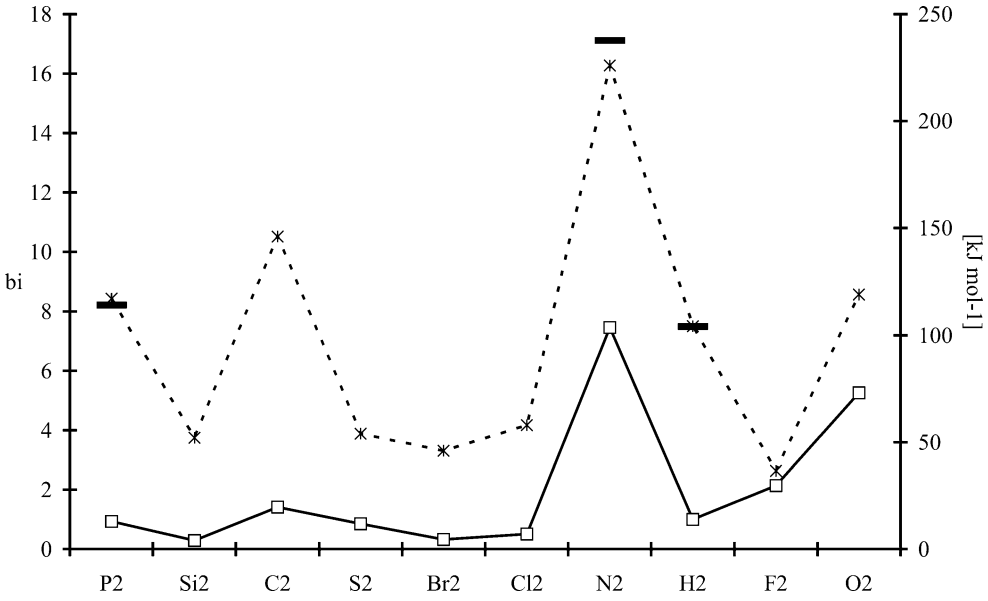

Fig. 3 Correlation of b_ε (squares) and $b_{\Delta\varepsilon}$ (strokes) with standard bond energies [kJ mol^{-1}] taken from literature [40] (doted line). The $b_{\Delta\varepsilon}$ has been normalized to level of H_2 standard bond energy. The molecules are ordered according to the increasing largest eigenvalue of stress tensor at Lagrange point (from left to right)

Energy density in real space

The electronic stress, kinetic energy density and interaction energy density may be represented in real space providing a more detailed and prospective view that complements the information obtained from Lagrange point. In the case of interaction energy density real space data is especially valuable showing the source of stability or weakness of molecules.

Figure 4 shows redistribution of interaction energy density in space while the electron density change in space is shown in Fig. 5. The metal atoms from first group constitute bonds with wide stabilization regions (represented by blue isosurfaces) in between atoms and wide destabilization regions outside. The region of negative interaction energy density that stabilizes the bond is in overlap with increased electron density regions (represented by red isosurfaces in Fig. 5). The second group elements have bonds very similar to H_2 bond, where both atoms are buried in the stabilization region that spreads around the whole molecule. However in the case of these elements the negative interaction energy density region is redistributed over the much larger space and energetically unfavorable regions are limited only to doughnut structures surrounding the bond. One can notice that electron density increase between atoms is limited to small σ-like region while outside interatomic region it is widely redistributed. On the other hand the hydrogen molecule is closed in shell structure in which the center is formed by stabilized core of increased electron density. The N_2 and P_2 molecules show stability in "σ*" shaped region surrounded by stabilization ring. The As_2 molecule, in contrast to former ones, innermost has σ like stabilization region submerged in bulk of destabilization. The negative interaction energy density regions usually cover the electron density increase regions. However this is not exactly the case for H_2 and N_2 molecules for which regions of favorable interaction also appear in places where electron density is decreased. This may have connection with greater stability (and lower reactivity, see $b_{\Delta\varepsilon}$ parameter in Table 2) of these molecules comparing to the other species from the given group in periodic table.

Figures 6 and 7 present visualization of interaction energy density and electron density change for noble gases. The magnitude of interaction energy density is very small (almost in error limit) however one can notice for interatomic region that the stabilization effect occurs due to decrease of electron density in this region (in contrast to other molecules where attractive interaction energy density comes in pair with increase of electron density). Among all noble gases species the Ne_2 is characterized by strongest interaction (greatest b_i indices). The source of such stability might be explained by the following issues. The Ne_2 has the shortest optimized interatomic distance of all presented noble-gases, very close to that in Na_2. Although the electron density at Lagrange point has been decreased about two orders more then for other noble-gases, still it's value is an order greater then others. The strong accumulation of electron density on atomic cores is also observed with very small and diffused destabilization in those regions.

Conclusions and discussion

The supermolecular approach when applied to diatomic molecules needs to take into account the possible electronic configurations and orbitals orientations for atomic mono-

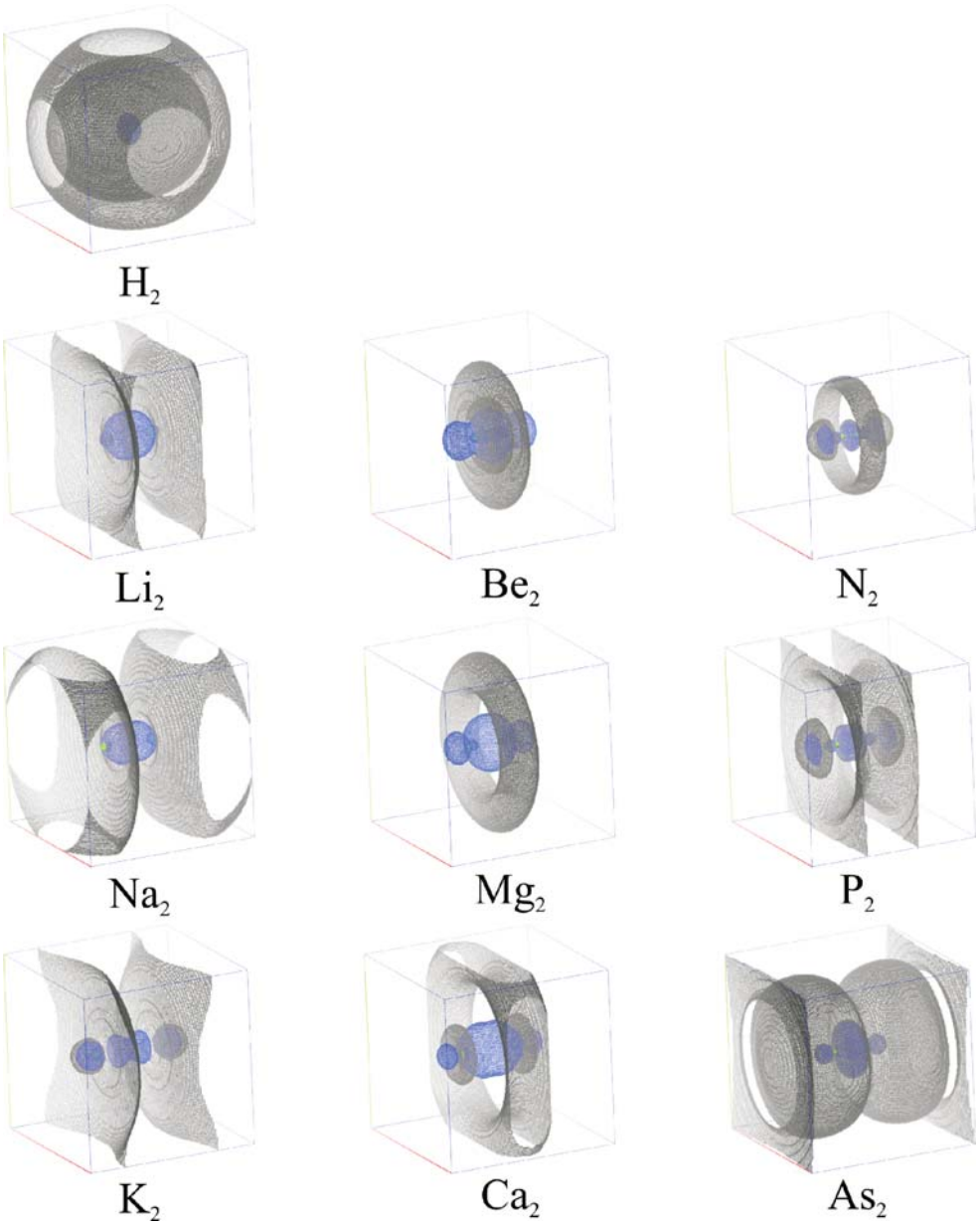

Fig. 4 Interaction energy density. Black isosurfaces correspond to zero value of interaction energy density. The blue regions mark out the negative interaction energy density space $\Delta\varepsilon^{S}_{\tau AB}(\vec{r}) < 0$; in the complement space $\Delta\varepsilon^{S}_{\tau AB}(\vec{r}) > 0$. The diameter of cube is 20 bohr. The atoms represented by green CPKs [41]

mers. In the case of diatomic species of 3rd, 4th, 6th, and 7th group elements a more careful and detailed analysis is required, which has not been applied on this stage yet. Some difficulties are originated from single determinant wave function, utilization of which causes no reasonable orientations of atomic orbitals of monomers in some atoms that do not correspond to ones in dissociation limit (configuration of maximum overlap in molecule). We need to revise our definition of atomic monomer in some cases. Nevertheless the method for obtaining the three-dimensional interaction energy density in the present state is fully applicable to intermolecular interactions, in generic circumstances.

Lagrange point is the characteristic point of bond line that may represent bond properties using energy density data. The total energy density (calculated as the trace of stress tensor) is in close association with electronic and chemical properties of molecules. It is possible to characterize interactions and to evaluate their strengths and energy based bond orders using the energy density related indices. However we need a more detailed study to find the source of difference between values of bond orders calculated in our method with commonly used ones. The correspondence of b_{ε}, b_{μ} and $b_{\Delta\varepsilon}$ indices describing reactivity with standard bond energies was found and only small basis set and immaterial method dependency of these indices have been inferred. However a single point is not enough for full characterization of bonding interactions. The three-dimensional insight is much more informative. The differences in

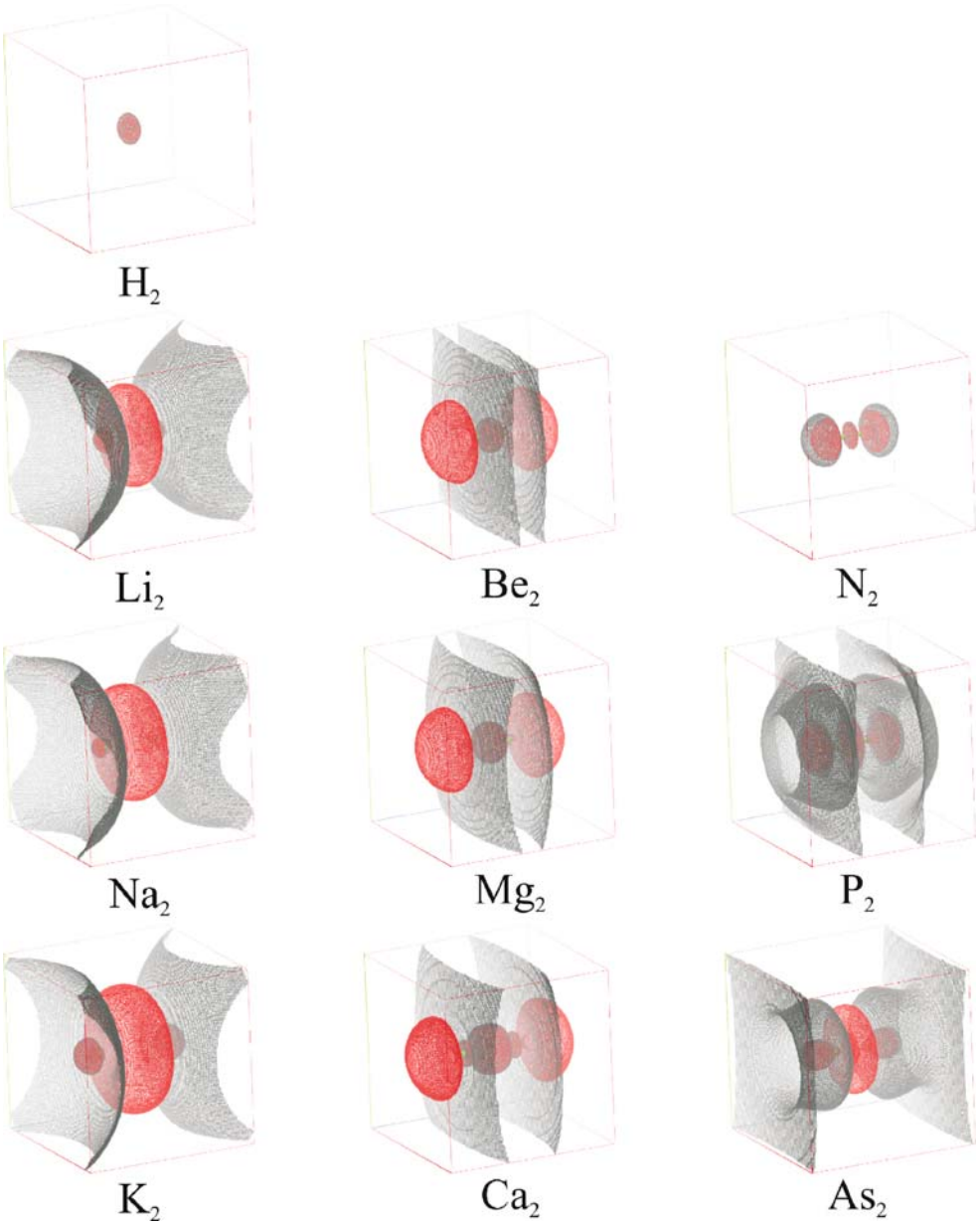

Fig. 5 Electron density redistribution change calculated as difference of molecule and atoms electron densities. Black isosurfaces correspond to zero value. The red regions mark out the regions of increased electron density $\Delta n_{AB}(\vec{r}) > 0$; in the complement space $\Delta n_{AB}(\vec{r}) < 0$. The diameter of cube is 20 bohr. The atoms represented by green CPKs [41]

the redistribution of interaction energy densities are in close relation with activity of a given molecule. Furthermore it may provide details on orbital interaction, spin state and stability of a given compound.

It may seem strange that the values of the b_μ index calculated for noble-gas diatomic molecules are surprisingly large in some cases (the He_2, Ne_2, Ar_2, Kr_2 values are larger than Li_2, Na_2, K_2), while the b_ε index gives practically zeros. In fact all noble gases dimers have very low b_ε indices (except Ne_2 for which it is comparable to that of Na_2 or K_2), which indicates very weak bonding. However the greater b_μ index is associated with greater absolute value of local chemical potential of bonded atoms that is the potential of electrons to undergo physical or chemical change in the system. The similar points (competition between stabilization energy and chemical potential) may also apply to other species, i.e., of fifth group (N_2, P_2, As_2) explaining it's reactivity and the deviation of b_ε from commonly used bond orders. In addition in the presented set of molecules only noble gases have negative kinetic energy density at Lagrange point. The atoms and interatomic region of bonded molecules are embedded in positive kinetic energy density region. The noble gases atoms (positive kinetic energy density) are separated and surrounded by negative kinetic energy density without any connection in shape of positive region, which reflects a leading role of long range field (electrostatic or quantum in nature) effects for interaction between noble gases. Although we have found very little method dependency, the HF level is not suitable for noble gases calculations. The noble

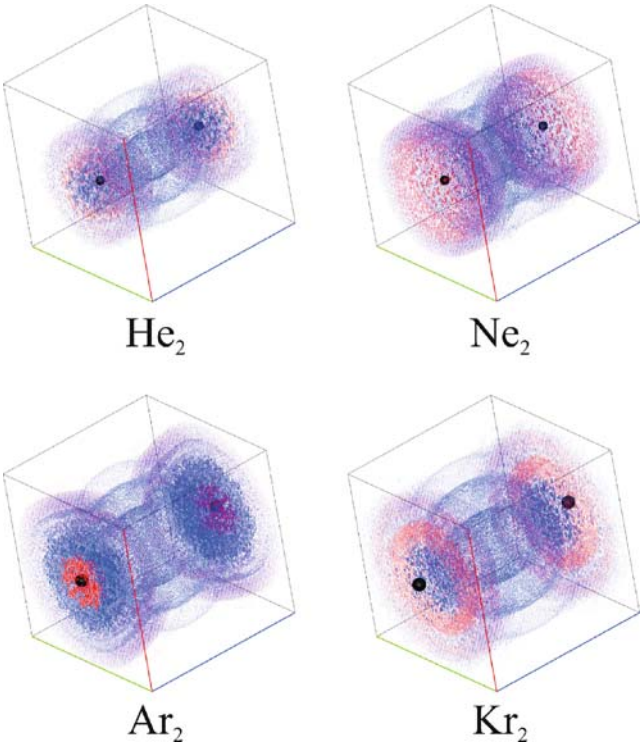

Fig. 6 Interaction energy density-noble gases: the blue dots represent the negative interaction energy density space; the red dots-positive. The size of dots corresponds to the magnitude of energy density. The diameter of cube is 20 bohr. The atoms represented by black spheres [41]

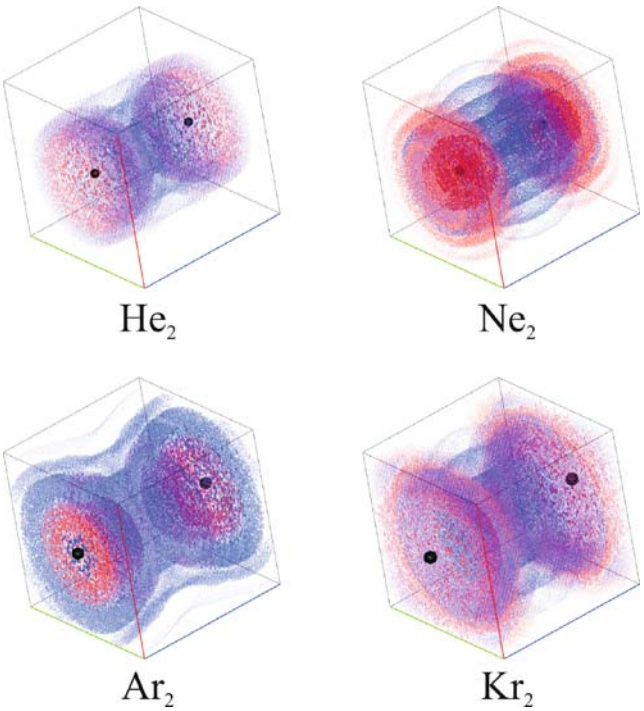

Fig. 7 Electron density redistribution change (noble gases) calculated as difference of molecule and atoms electron densities. The red dots show increased electron density; the blue dots apply to decreased electron density. The size of dots corresponds to the magnitude of electron density change. The diameter of cube is 20 bohr. The atoms represented by black spheres [41]

gases have one of the lowest bond order indices. The use of a more sophisticated method and inclusion of higher dispersion and correlation effects should lead to more accurate results in this case.

Another unusual result is that the P_2 molecule shows a substantially different figure of bond order from MO-based bond order. The Table 4 compares molecular orbitals energy densities in Lagrange point of three "triple bonded" molecules. The N_2 has the lowest energy in Lagrange point for all highest occupied molecular orbitals, filled by valance electrons (except σ*) and the lowest sum of energies of MO-s of core electrons. Second is carbon-carbon bond in C_2H_2 and P_2 at the end. Our bond orders give the same order of decreasing bond order. The interatomic distances are: 1.07[Å], 1.18[Å], and 1.85[Å], respectively. The electron density decreases with increasing distance. One should notice that our indices are deeply related to electron density accumulated in meta-stable position at Lagrange point and its energy not only in the total effect.

There are many discussions in literature about bonding itself and some research works even claim that there is no such thing as a chemical bond at all. The new indices, although they reflect traditional bond orders, are carrying different information about interactions on the interfaces of quantum chemical subsystems. Thus we can not judge and recommend one of our new indices as representative method to estimate bond order. Our indices satisfy the earlier definition of bond order (by IUPAC) as "index of the degree of bonding between two atoms relative to that of a single bond". The bond order is provided by energy density associated with localized electron density, as the combined effect of all occupied molecular orbitals (which in some part corresponds also to molecular-orbital bond order definition). Since electronic energy density includes the electronic spin angular momentum in the underling physics, so does the energy density based bond order. However depending on the specific information one may use either one or all new indices to characterize molecules and chemical interactions.

Table 4 The energy densities [au/bohr^3] at Lagrange point $\vec{r}_{Lagrange}$ for highest occupied molecular orbitals

MO	N_2	C_2H_2	P_2
π (HOMO)	−0.3174	−0.1440	−0.0320
π (HOMO)	−0.3174	−0.1440	−0.0320
σ	−0.5567	−0.2632	−0.0955
σ*	−0.0022	−0.0013	−0.0061
σ	−0.8912	−0.3849	−0.0929
core	−0.0050	−0.0038	−0.0017

The core means sum of energy densities at $\vec{r}_{Lagrange}$ of core MO's. The valance electrons orbitals: σ-is sigma bonding MO, σ*-sigma antibonding MO, π-degenerated pi bonding MO.

Acknowledgements This work was supported by the Japanese Government-Monbukagakusho Scholarship through Kyoto University. The valuable discussions with Professor W. A. Sokalski and Dr. K. Doi as well as Dr. K. Doi and Mr. Y. Mikazuki for technical advice and support are acknowledged.

References

1. Tachibana A (1999) Theor Chem Acc 102:188–195
2. Tachibana A (1987) Int J Quantum Chem, Quantum Chem Symp 21:181–190
3. Tachibana A (1996) Int J Quantum Chem 57:423–428
4. Tachibana A, Parr RG (1992) Int J Quantum Chem 41:527–555
5. Tachibana A, Nakamura K, Sakata K, Morisaki T (1999) Int J Quantum Chem 74:669–679
6. Bingel WA (1963) Z Naturforsch A 18A:1249–1258
7. Bingel WA (1967) Theor Chim Acta 8:54–61
8. Kato T (1957) Commun Pure Appl Math 10:151–171
9. Pack RT, Brown WB (1966) J Chem Phys 45:556–559
10. Tachibana A (2001) J Chem Phys 115:3497–3518
11. Hohenberg P, Kohn W (1964) Phys Rev 136:B864–B871
12. Mermin ND (1965) Phys Rev A 137:1441–1443
13. Parr RG, Yang W (1989) Density functional theory of atoms and molecules. Oxford University Press, New York
14. Tachibana A (2002) Energy density in materials and chemical reaction systems. In: Sen KD (ed) Reviews in modern quantum chemistry: a celebration of the contributions of Robert Parr, vol 2. World Scientific, Singapore, pp 1327–1366
15. Tachibana A (2005) J Mol Model 11:301–311
16. Tachibana A (2004) Int J Quantum Chem 100:981–993
17. Tachibana A (2003) Field energy density in chemical reaction systems. In: Brändas E, Kryachko E (eds) Fundamental perspectives in quantum chemistry: a tribute to the memory of Per-Olov Löwdin, vol 2. Kluwer, Dordrecht, pp 211–239
18. Tachibana A (1991) J Math Chem 7:95–110
19. Tachibana A (1994) String Model of Chemical Reactions. In: Kryachko ES, Calais JL (eds) Conceptual trends in quantum chemistry. Kluwer, Dordrecht, pp 101–118
20. Fukui K (1970) J Phys Chem 74:4161–4163
21. Fukui K (1981) Acc Chem Res 14:363–368
22. Tachibana A (1999) Electronic energy density in chemical reaction systems. In: Fueno T (ed) The transition state-A theoretical approach. Kodansha, Tokyo, pp 217–247
23. Bader RFW (1990) Atoms in molecules-A quantum theory. Oxford University Press, Oxford
24. Frisch MJ, Trucks GW, Schlegel HB, Scuseria GE, Robb MA, Cheeseman JR, Montgomery JA, Vreven JrT, Kudin KN, Burant JC, Millam JM, Iyengar SS, Tomasi J, Barone V, Mennucci B, Cossi M, Scalmani G, Rega N, Petersson GA, Nakatsuji H, Hada M, Ehara M, Toyota K, Fukuda R, Hasegawa J, Ishida M, Nakajima T, Honda Y, Kitao O, Nakai H, Klene M, Li X, Knox JE, Hratchian HP, Cross JB, Bakken V, Adamo C, Jaramillo J, Gomperts R, Stratmann RE, Yazyev O, Austin AJ, Cammi R, Pomelli C, Ochterski JW, Ayala PY, Morokuma K, Voth GA, Salvador P, Dannenberg JJ, Zakrzewski VG, Dapprich S, Daniels AD, Strain MC, Farkas O, Malick DK, Rabuck AD, Raghavachari K, Foresman JB, Ortiz JV, Cui Q, Baboul AG, Clifford S, Cioslowski J, Stefanov BB, Liu G, Liashenko A, Piskorz P, Komaromi I, Martin RL, Fox DJ, Keith T, Al-Laham MA, Peng CY, Nanayakkara A, Challacombe M, Gill PMW, Johnson B, Chen W, Wong MW, Gonzalez C, Pople JA, (2003) Gaussian 03, Revision C.02, Gaussian, Inc., Wallingford CT
25. Nakamura K, Doi K, Tachibana A, MRDFT program; available on request via e-mail: akitomo@scl.kyoto-u.ac.jp
26. Mayer I (1983) Chem Phys Lett 97:270–274
27. Mayer I (1985) Tcheoret Chim Acta (Berl.) 67:315–322
28. Mayer I (1986) Int J Quantum Chem 29:73–84
29. Mayer I (1986) Int J Quantum Chem 29:477–483
30. Mulliken RS (1955) J Chem Phys 23:2343–2346
31. Ruedenberg K (1962) Rev Mod Phys 34:326–376
32. Roby KR (1974) Theor Chim Acta 33:105–113
33. Coulson CA (1939) Proc Roy Soc A 169:413–428
34. Coulson CA (1961) Valence, 2nd (edn). Clarendon Press, Oxford
35. Onsager L (1931) Phys Rev 37:405–426
36. Onsager L (1931) Phys Rev 38:2265–2279
37. Herring C, Nichols MH (1949) Rev Mod Phys 21:185–270
38. Groot SR, Mazur P (1984) Non-equilibrium thermodynamics. Dover Publications Inc., Dover Ed edition, pp 339–345
39. Boys SF, Bernardi F (1970) Mol Phys 19:553–556
40. Atkins P, de Paula J (2006) Atkins' physical chemistry, 8th edn. Oxford University Press, New York, pp 1011–1012
41. Humphrey W, Dalke A, Schulten K (1996) J Molec Graphics 14:33–38 (http://www.ks.uiuc.edu/Research/vmd/)